

Three-Dimensional Electronic Surfaces

J.C. Sturm, P.I. Hsu, S.M. Miller, H. Gleskova, A. Darhuber, M. Huang, S. Wagner, S. Troian, and Z. Suo

Center for Photonics and Optoelectronic Materials (POEM), Princeton University,
Princeton, NJ 08544 USA

609-258-5610, 609-258-1954, sturm@ee.princeton.edu

Abstract

There is an increasing interest in electronics functionality on surfaces which are not planar. This paper examines the critical technologies for fabricating electronic surfaces which have a three-dimensional shape. Two different approaches for achieving such a goal are examined. One can fabricate electronics using conventional technologies on a flat surface, and then after fabrication deform that surface into the desired shape (e.g. a spherical cap). In an alternative approach, one can directly fabricate onto substrates with an arbitrary shape. In this case one must address the issue of pattern formation and transfer on the curved surfaces. The scaling of letterpress printing to micron-scale features on flat and spherically curved surfaces is demonstrated.

Introduction

Electronic and optoelectronic products are conventionally flat because of their fabrication on the surface of a semiconductor wafer or glass. However, there are several drivers for curved products. A straightforward example would be a flat panel display which could be rolled up. A more complex example might be an artificial "sensitive skin" which could be worn over a robot surface for collision avoidance or on a person as a medical monitoring device. Finally, for focal plane array imagers with large fields of view, the optics to provide a spherically curved focal plane (as opposed to a conventional focal plane) are far smaller, translating into a smaller, lighter, and lower cost system. Thus one wants a similarly curved detector array. This paper will specifically address the fabrication of a product which might have a complex surface shape, but would not have to change shape during use.

In making such a surface in three dimensions which has electronic capability, one could consider making it first on a flat substrate (such as a metal or plastic foil) and subsequently deforming the processed substrate to the final shape. This approach has the benefit of relatively straightforward device fabrication on a planar surface, but the deformation could damage the fabricated components or interconnects. The first part of this paper explores the limits of this approach. The second part of the paper examines a printing technology which might be applied to define patterns directly on curved surfaces of arbitrary shape. With such a technology one could then consider device fabrication directly on the curved surface. The scaling of letterpress printing on planar and curved surfaces is examined.

Deformation of Prefabricated Planar Substrates

Spherical Deformation

As a model system, we considered the deformation of prefabricated substrates into the shape of a spherical cap. Both stainless steel foil and polyimide foil substrates were examined. The deformation was experimentally accomplished by clamping the circular edge of the foil fixed (diameter 5-8 cm) and then deforming the substrate by applying gas pressure under the foil (Fig. 1). Both steel and polyimide substrates (thicknesses from 20 to 50 microns) could easily be deformed into a spherical shape with this method with gas pressures in the range from 10 to 50 psi [1]. To convert from a flat surface into a spherical cap shape, it is clear that the surface must be stretched. From geometrical arguments it can be shown that for thin substrates, average radial strain $\epsilon_{r,avg}$ over a line through the center of the foil depends only on the angle θ which the spherical cap subtends:

$$\epsilon_{r,avg} = \frac{\frac{\theta}{2} - \sin \frac{\theta}{2}}{\sin \frac{\theta}{2}} \approx \frac{\theta^2}{24} \quad (1)$$

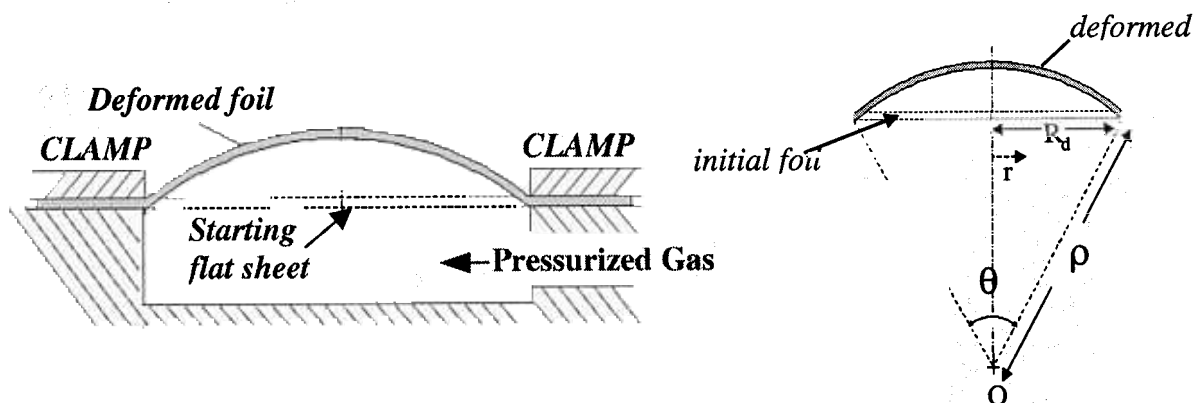


Figure 1. Schematic diagram indicating apparatus for deforming thin foil substrates, and definition of subtended angle θ after fabrication.

If one has a target subtended angle of 66° , corresponding to a solid angle covered by the cap of one steradian, the average radial strain is 5.6%. Such a strain is beyond what is generally achievable by purely elastic deformation with substrate materials such as plastic or metal, so that plastic deformation will occur and the foil will be permanently deformed. For such deformations which encompass a solid angle of ~ 1 steradian, the final resulting shapes are indeed spherical within experimental resolution. The resulting strains of $\sim 5\%$ are larger than the fracture limits of brittle device materials such as silicon, silicon dioxide, silicon nitride, etc, which are on the order of 1% or less. Therefore if there is a continuous thin film of such material (e.g. SiO_2) deposited on the substrate before deformation, it will crack as it is put in extreme tension as the substrate

is expanded. Thus the cracking of inorganic semiconductor device materials is the first order problem which must be addressed for the post fabrication deformation of finished foils.

To overcome the problem of keeping previously fabricated thin film semiconductor devices on top of the substrate from cracking when the substrate is deformed, islands of "hard" semiconductor device material (100 nm of amorphous silicon on top of 400 nm of silicon nitride) were patterned on top of a "soft" polyimide substrate before deformation [1]. For comparison, the Young's moduli of silicon and polyimide are ~ 200 and ~ 5 GPa, respectively. Furthermore, plastic flow in the polyimide begins already at a very low strain. Therefore the substrate can deform and then flow under the island as the foil is deformed, minimizing the strain in the island and preventing it from cracking.

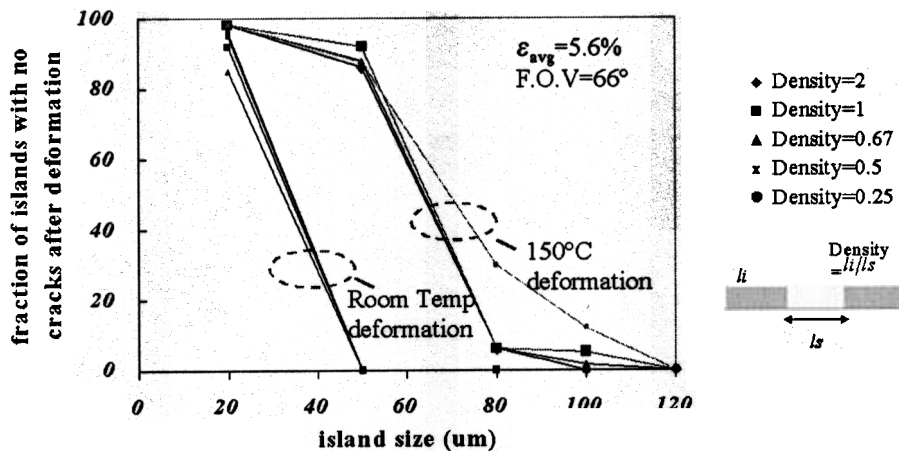


Figure 2. Yield of uncracked islands of 100 nm a-Si/400 nm Si_3N_4 on polyimide after expanding to 66° field of view (average strain of 5.6%) at room temperature and 150 °C, for different island densities. Island density is defined as the island edge over the island spacing [1].

Both numerical modeling and experiments show that the strain increases with the island size. Thus smaller islands remain intact for a given deformation while larger islands crack (Fig. 2). The critical island size at which islands fail is larger for higher deformation temperatures because the polyimide softens at higher temperature. For deformation at 150 °C, a very high yield of 50-micron islands can be obtained. (Fig. 3 shows a micrograph of such islands of varying size on a deformed piece of polyimide. Current research involves the fabrication of TFT's and circuits in the islands before deformation, and studying the effect of the deformation on their performance).

The critical tensile strain in the islands before they break during expansion can be inferred by comparing the size at which they tend to break (Fig. 2) with the maximum strain in the islands found by numerical simulation of the strain fields resulting from deformation. This is found to be $\sim 0.5 - 0.8 \%$. Since the average strain across the foil is $\sim 5-6\%$ (by geometrical considerations), this implies that the strain between the islands is much larger than 6%. This means there is considerable plastic flow of the substrate

between the islands. This extreme plastic flow between the islands qualitatively explains the fact that the yield of the islands without cracks depends only very weakly on how far apart the islands are placed, a beneficial effect. However, because the strain is so large between the islands, the strain on any interconnects between islands in these regions will be enormous, and without special measures it is likely that such interconnects would fail. The fabrication of patterned metal layers on curved surfaces as a route to achieving interconnects will be investigated in the next section of the paper.

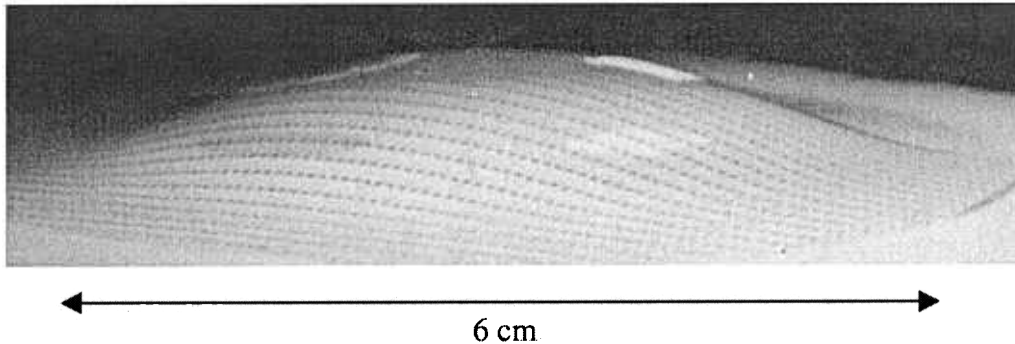


Figure 3. Picture of polyimide foil with a-Si/Si₃N₄ islands after deformation to a spherical cap shape with a ~66° field of view.

Cylindrical Deformation

To further investigate the maximum tensile strain which amorphous silicon device structures can withstand before immediate failure, bottom-gate a-Si TFT's were fabricated on a Si₃N₄ buffer layer on 50-micron polyimide foils [2] or 10-20 micron stainless steel foils (with an oxide passivation layer) [3]. They were then deformed by cylindrically deforming them with various radii of curvature (down to ~0.5 mm) [4,5]. When a thin film substrate is cylindrically deformed, the inside surface of the foil is in compression and the outside surface is in tension. If the mechanical stiffness of the TFT layers on the surface is small compared to that of the substrate [9], it is well known that for a radius of curvature ρ , the magnitude of the strain ϵ on the two surfaces is

$$\epsilon = t / 2\rho \quad (2)$$

where t is the thickness of the foil. Thus, unlike spherical deformation, the strain can be made small by reducing the substrate thickness. Therefore with thin substrates of a flexible foil, several groups have demonstrated devices or circuits which can be deformed in one dimension [6-8]. For Eq'n. [2], or a more complicated expression if the substrate is compliant compared to the surface layers [9], one knows the strain in the TFT layers as a function of the bending radius. TFT's were measured before and after the cylindrical deformation (and release).

Fig. 4 shows the results for TFT's on the polyimide foils subjected to compression (inside surface during curvature) or to tensile stress (outside curvature). Under tension, a change in the TFT characteristics was observed beginning at a radius of 2 mm,



corresponding to 0.5% tensile strain. Under SEM inspection, the failure mode was observed to be cracking, which is expected to relieve tensile strain. This 0.5% limit is similar to the tensile strain limit observed before cracking in the case of spherical deformation of a similar materials stack.

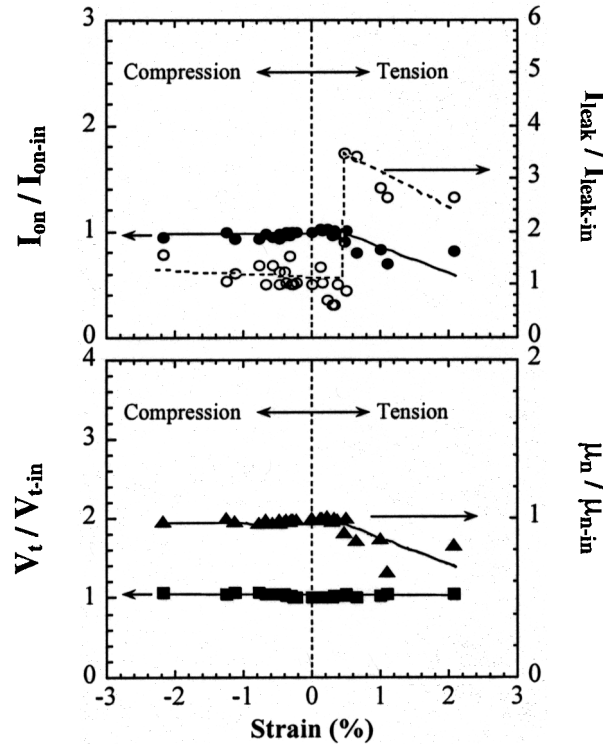


Figure 4. Transistor parameters of a-Si TFT's on 25-micron polyimide substrates after one minute of cylindrical deformation and release, normalized to their values before deformation [5].

Wet Printing for Device Fabrication

The goal of printing as it relates to device fabrication is to create low cost methods for fabricating microstructures on large area substrates. Traditional printing techniques are excellent for creating patterns of ink with sizes 100 μm and larger. In order for printing technologies to be truly useful for device fabrication, however, feature sizes must be reduced to at least the micron scale. To address this issue, new microfabrication techniques, so-called soft-lithography techniques, have been developed recently [10,11] and used to produce parts of functioning electronic devices [12]. These techniques approach microfabrication and nanofabrication in non-traditional ways, replacing photolithography with printing and molding techniques. Furthermore, as we will demonstrate, these techniques can also be used for pattern definition on non-planar surfaces for which optical lithography is ill-suited.

The “inks” commonly printed with soft lithographic techniques are so-called self-assembled monolayers [10]. Such monolayers have been shown to function as etch masks for certain wet etching processes [10], but these printed monolayers cannot serve as etch resist for more aggressive plasma etching processes. Also, since the self-assembly processes used in these techniques can be dependent on substrate surface chemistry, they are not suitable for arbitrary substrates and may not be suitable for all applications.

We seek to develop general micropatterning techniques for device fabrication based on wet printing of polymers, similar to techniques used for ink-printing in the macro-world. We use the term “wet printing” to differentiate these techniques that printing fluid inks from the printing of monolayers or colloidal particles. Such printing methods, using polymer inks, will not rely on sensitive chemical or physical properties of the workpiece onto which materials are to be printed, and should give maximum flexibility in terms of further processing. We believe wet printing techniques will be used in the future to print active device materials, such as conductors, semiconductors, and insulators.

Polymer Wet Printing Techniques

One of the great challenges facing the application of wet printing for device fabrication is improving printing resolution. There are several styles of printing that can be adapted for high-resolution printing of polymers. The techniques vary most notably by the method used to confine the ink on the printing plate. Figure A illustrates four printing styles [13] that have been investigated for device fabrication. *Gravure* printing (Fig. 5(a)) employs a topologically patterned printing plate with grooves defining regions for ink placement. The ink is deposited onto the entire plate and wiped away from all raised surfaces, leaving ink confined only in the grooves. Gravure printing has been used to fabricate functioning transistors by printing resist layers with minimum printable line widths of approximately 45 μm [14]. By patterning the transistor channel as the space between two printed lines, the minimum channel length of these transistors was 10 μm . More recently, gravure printing has been used to print 50 μm patterns of conducting pastes [15]. *Imprinting* (Fig. 5(b)) also utilizes a printing plate patterned with grooves defining the desired ink placement. With imprinting, however, the ink is applied to the workpiece rather than the printing plate, and then the printing plate is used to squeeze the ink away from undesired areas. A variation of this technique, nanoimprint lithography, has been used to produce 25 nm lines and dots [16] in etch resist polymers and has been applied to large areas [17], although it requires high pressures to achieve acceptable pattern reproduction. Unlike the preceding techniques, *offset* printing (Fig. 5(c)), does not rely on a surface topology pattern to confine the printing ink. Instead, the surface energy of the printing plate is patterned using very thin films, to define wetting and non-wetting regions for the ink. Because the chemical pattern is very thin compared to the deposited ink, the printing plate can be treated as flat. This technique has been the subject of much recent investigation [18-21], using self-assembled monolayers to define the wetting regions, and has been demonstrated capable of printing patterns with feature sizes less than 10 μm .

Finally, *letterpress* printing (Fig. 5(d)), for which we are presenting the first micro-scale investigation, is almost the inverse of the gravure technique. This technique uses a topologically patterned printing plate, but deposits the ink onto the raised features and does not require removing excess ink from the printing plate. In this way, the process resembles rubber-stamping, with the resolution improved by several orders of magnitude. Schematically this also resembles microcontact printing [10], with polymer inks replacing monolayer inks.

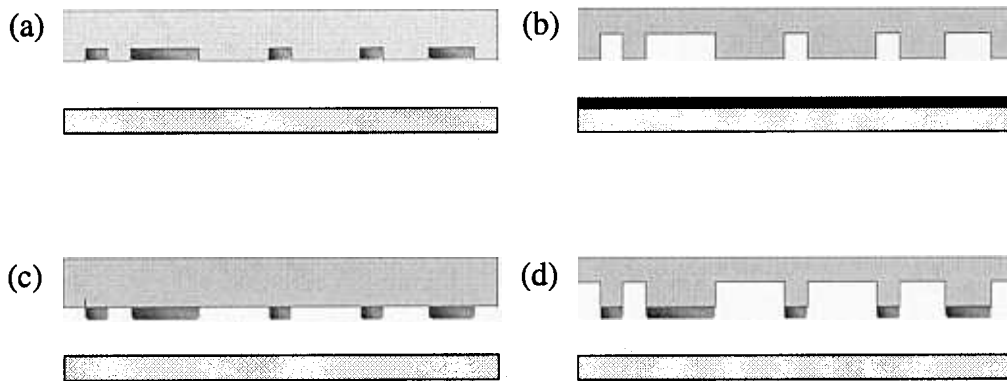


Figure 5. Four printing techniques. Each panel shows a printing plate above a workpiece prior to printing, with the location and conformation of the ink indicated. (a) gravure printing, (b) imprinting, (c) offset printing, and (d) letterpress printing.

Letterpress Printing Plate Fabrication

The printing plate used for our letterpress printing process is typically referred to as a stamp, by analogy to rubber stamps. Preparation of these stamps generally involves two major steps: (1) application and patterning of an etch mask on the stamp substrate, and (2) anisotropic etching of the stamp substrate to create the topological pattern. The pattern created in the first step is a positive image of the pattern that will be printed using this stamp. The printing stamps were prepared primarily from silicon wafers as rigid stamps and from Kapton (polyimide) foils as soft and flexible stamps that allow us to print onto flat, cylindrical, or spherical surfaces. For both materials, 200 nm of silicon nitride was deposited by plasma enhanced chemical vapor deposition (PECVD) and then patterned by conventional lithography and dry-etching. The nitride served as a mask for a wet etch (for Si) or dry etch (for polyimide) to etch the substrate 5-10 microns deep to create the stamp topology. The nitride was left on the raised features after etching.

Letterpress Printing Process

The process used for letterpress printing of polymers consists of two steps (Fig. 6). First, the polymer ink is applied selectively to the raised features on the stamp, and second, this polymer is printed onto a workpiece. After printing, polymer remaining on the stamp can be removed with solvent and the stamp can be reused; we have not

observed stamp degradation with repeated use. In order to use the printed polymer in device fabrication, the polymer must be a solid under further processing conditions. But for wet printing to be successful the polymer must be fluid during the printing process. To achieve this, we have used a thermoplastic polymer ink and carried out the printing process above its glass transition temperature, but we have done all subsequent processing below this temperature. One of our objectives was to use the printed polymer as an RIE resist, so we chose polystyrene as our ink; the high carbon atom fraction in polystyrene leads to good dry etch resistance [22,23]. Since we wanted a low viscosity polymer ink during printing, we chose polystyrene molecular weight, M_w , below the entanglement molecular weight, M_e , ($M_w = 0.8\text{-}5 \text{ kg/mol}$, $M_e = 18 \text{ kg/mol}$) and carried out the printing process above the glass transition temperature, T_g , ($T_{\text{process}}=180 \text{ }^\circ\text{C}$, $T_g=95 \text{ }^\circ\text{C}$).

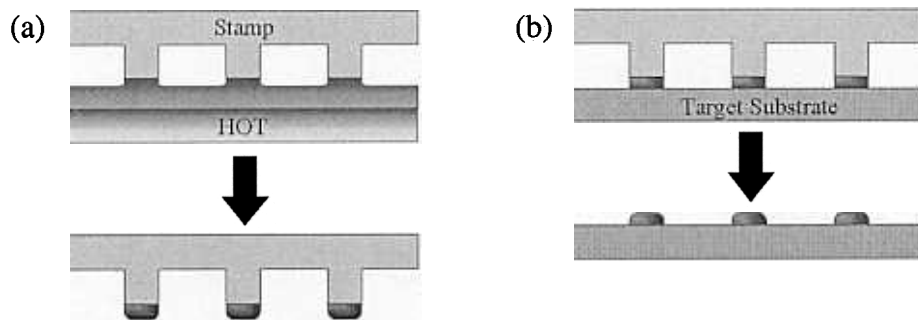


Figure 6. Letterpress printing process. (a) The polymer ink is applied to the stamp by the melt transfer process. (b) The polymer is printed onto the workpiece by a similar melt transfer process.

In the first printing step, the polymer ink is applied to the stamp by a melt transfer process wherein the stamp contacts a thin film polymer melt on a solid surface, eg. glass. This thin polymer film is previously deposited by spin coating the glass with a polymer solution and heating to evaporate any residual solvent; toluene is used as the solvent for polystyrene. The thickness of this film can be controlled and is usually in the range of 500 nm to 1 μm . The melt transfer process is performed by heating the uniformly coated substrate to the process temperature on a hotplate and then placing the stamp face-down onto this substrate. The polymer deposited on the stamp has a typical average thickness of 200 – 400 nm, which is independent of feature size. Fig. 7 (a) shows a typical stamp after polymer deposition.

In the second printing step, the polymer ink is printed from the stamp to the target workpiece by repeating the melt transfer process used to ink the stamp. Either the stamp or workpiece is heated on a hotplate to the process temperature and then the other is pressed into contact and peeled off. The typical printed film thickness is 100 – 200 nm. The film thickness is relatively uniform across a single sample and is independent of feature size. Fig. 7(b) shows 15 μm polystyrene squares printed onto a silicon nitride coated silicon wafer (200 nm by PECVD). The optical interference fringes observed in the micrograph indicate that the printed polymer structures are not flat, but are instead

domed. This is because surface tension acts to minimize the surface energy and tends to round the structures [18], eventually creating spherical cap profiles if the polymer is allowed to fully redistribute before solidification. For large features it is typically observed that the surface profile is locally smooth but uneven on longer length scales; thicker mounds of polymer are distributed within the thin film. These non-uniformities are due to a viscous fingering instability in the fluid transfer that is not observed for small features because the feature size is below the wavelength of the instability [19].

The polymer structures we have made by letterpress printing have been used as masks for both wet and dry etching processes. Fig. 7(c) shows 15 μm silicon nitride squares which were created by reactive-ion etching in the sample of Fig. 7(b). The polystyrene shows good etch resistance for this process. The micrograph in (d) shows 2 μm gold circles created by printing polystyrene masks onto a 100-nm gold film and 10-nm chromium adhesion layer, which were wet etched using the printed polystyrene mask.

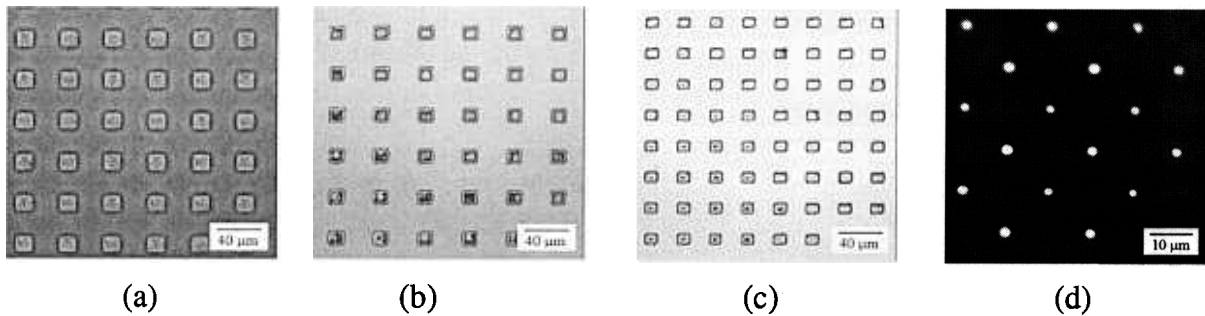


Figure 7. Optical microscope images of the letterpress printing process: (a) the stamp with polystyrene deposited on the raised structures, (b) patterned polystyrene on Si_3N_4 -coated wafer, (c) sample of (b) after Si_3N_4 etching, and (d) 2- μm and 4- μm diameter gold dots patterned by letterpress printing.

Despite the variations in local film thickness that are observed for large features, the average printed film thickness is independent of feature size, and many sizes of features can be printed simultaneously with this technique; this has been shown to be difficult for some other printing techniques [18]. Using letterpress printing, we have fabricated microstructures as small as 2 μm and simultaneously printed structures as ranging from 15 μm to 150 μm . We are currently investigating some resolution-limiting phenomena such as spreading of the printed polymer micro-droplets and pattern fidelity reducing phenomena such as the rounding of sharp corners.

Printing on Curved Surfaces

In the first part of the paper we discussed the desire to fabricate interconnects on curved surfaces after the substrate foils with device islands have been deformed. In this section, we describe the application of letterpress printing to pattern definition on a spherically-curved surface, and the patterning of metal layers with this method. In our process, we first deform a thin foil target workpiece, typically Kapton, into the shape of a

spherical cap. We then make a hole at the apex of this cap to allow air to escape during the subsequent printing step, as shown in Fig. 8(a) (although this step would not be necessary if the process were done in a vacuum). Next, the pre-inked deformable polyimide letterpress stamp is loaded into the deformation apparatus (Fig. 1) with the raised features facing up. The spherical workpiece is placed above the stamp, with the concave side facing down, and the two are clamped in position. The printing is accomplished, as illustrated in Fig. 8(b), by increasing the air pressure on the stamp's lower surface to achieve contact at the apex of the workpiece, which is observed to be the last point of contact. The sample is then heated to transfer the polymer ink. The air pressure is decreased and the surfaces spontaneously separate as the elastic part of the stamp deformation relaxes. A spherically deformed stamp can be reused by re-applying ink with the same process used for printing, replacing the workpiece with a polymer-ink coated foil.

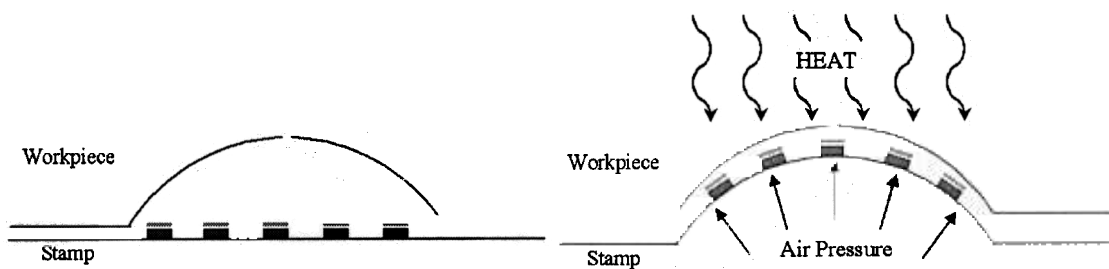
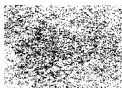


Figure 8: Schematic of the spherical printing process. (a) The workpiece and stamp prior to printing; the air release hole is indicated at the apex. (b) The workpiece and stamp during printing. In both panels the workpiece and stamp are in contact at the edges, the separation illustrated is only for graphical clarity.

Figure 9(a) shows a large-area view of polystyrene printed to the apex of a gold-coated, spherically deformed, Kapton foil. At the center of the image is the puncture hole that was made to allow the air to escape during printing. Fig 9(b) shows a magnified view of the smallest polystyrene features printed in this experiment; the designed pattern was $16\ \mu\text{m}$ squares. The printed features show some rounding because the workpiece was heated for some time after printing, allowing the polymer to spread. Fig. 9(c) shows the workpiece after etching the gold film as described for flat surfaces, and stripping the polystyrene. The shape of the metal features patterned on this spherical surface corresponds very well to that of the printed polymer. In addition to dots and squares, long lines (several cm) have also been successfully patterned. Further work is necessary to insure appropriate alignment of the mask and existing features on the target workpiece.

Summary

The mechanics of creating non-planar electronic surfaces, such as spherical caps and cylindrical shapes have been discussed. Cylinders can be achieved without damaging electronics on substrate surfaces by reducing the thickness of the substrate and using compliant substrates. However, for shapes such as spherical caps approaches such as device islands on soft substrates are required. While devices islands may be successfully deformed, the deformation of continuous interconnects will be more



difficult, and the patterning of metal which is deposited on a shaped surface may be required. Both for this application, as well as the low-cost patterning on flat surfaces, scaled approaches of letterpress printing have been investigated. A polymer layer of finite thickness is transferred, which may be used as a wet-etch or dry-etch mask for further processing. Two-micron and 15-micron features have been demonstrated on flat and curved surfaces, respectively.

This work was supported by the DARPA Molecular Level Printing and High Definition Display programs, and NJCST.

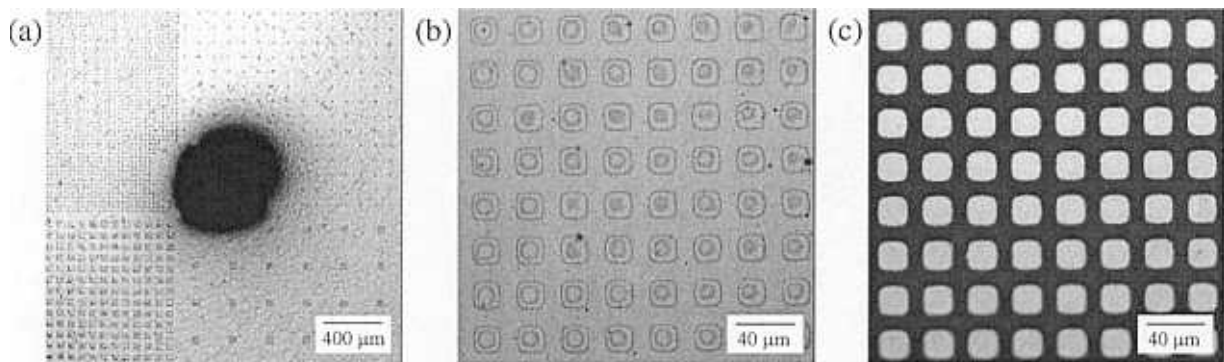


Figure 9: Optical micrographs showing a workpiece for spherical letterpress printing. (a) Polystyrene printed at the apex of a gold coated spherical Kapton foil, the dark spot at the center is the air-release hole. (b) A magnified view of part of panel (a). (c) The surface after metal etching polystyrene stripping.

References

1. P-H I. Hsu, M. Huang, S. Wagner, Z. Suo, and J.C. Sturm, Proc. Symp. Mat. Res. Soc. **621**, Spring 2000.
2. H. Gleskova, S. Wagner, and Z. Suo, Mat. Res. Soc. Proc. Symp. **508**, 73 (1998).
3. S.D. Theiss and S. Wagner, IEEE Elec. Dev. Lett. **17**, 578-580 (1996).
4. E. Y. Ma, S. D. Theiss, M. H. Lu, C. C. Wu, J. C. Sturm, and S. Wagner, Tech. Dig. Int. Elect. Dev. Mtg., 535-538 (1997).
5. H. Gleskova, S. Wagner and Z. Suo, Appl. Phys. Lett. **75**, 3011-3013 (1999).
6. D. B. Thomasson, M. Bonse, J. R. Huang, C. R. Wronski, and T. N. Jackson, Tech. Dig. Int. Elect. Dev. Mtg., 253-256 (1998).
7. G.N. Parsons, C.S. Yang, C.B. Arthur, T.M. Klein, and L. Smith, Mat. Res. Soc. Symp. Proc **508**, 19 (1998).
8. A. Constant, S. G. Burns, H. Shanks, A. Constant, C. Gruber, D. Schmidt, A. Landin, and F. Olympie, Proc. Electrochem. Soc. **96-23**, 382 (1997).
9. Z. Suo, E.Y. Ma, H. Gleskova and S. Wagner, App. Phys. Lett. **74**, 1177 (1999).
10. A. Kumar, H. A. Biebuyck, and G. M. Whitesides, Langmuir. **10**, 1498 (1994).
11. Younan Xia, and George M. Whitesides, Angew. Chem. Int. Ed. **37**, 551 (1998).
12. Zhenan Bao, John A. Rogers, and Howard Katz, J. Mater. Chem. **9**, 1895 (1999).



13. Michael H. Bruno, ed., Pocket Pal: A Graphic Arts Production Handbook, 16th ed., International Paper Company, 1995.
14. Yoshiro Mikami et al, IEEE Trans. Electron Devices **41**, 306 (1994).
15. M. Lahti, S. Leppävuori, and V. Lantto, Appl. Surf. Sci. **142**, 367 (1999).
16. Stephen Y. Chou, Peter R. Krauss, and Preston J. Renstrom, J. Vac. Sci. Technol. B, **14**, 4129 (1996).
17. Babek Heidari, Ivan Maximov, Eva-Lena Sarwe, and Lars Montelius, J. Vac. Sci. Technol. B **17**, 2961 (1999).
18. Anton A. Darhuber, Sandra M. Troian, Scott M. Miller, and Sigurd Wagner, J. Appl. Phys. **87**, 7768 (2000).
19. Scott M. Miller, Anton A. Darhuber, Sandra M. Troian, and Sigurd Wagner in Materials Development for Direct Write Technologies edited by D.B. Chrisey et al. (Mater. Res. Soc. Proc. **624**, Pittsburgh, PA in press).
20. Anton A. Darhuber, Scott M. Miller, Sandra M. Troian, and Sigurd Wagner in Materials Development for Direct Write Technologies edited by D.B. Chrisey et al. (Mater. Res. Soc. Proc. **624**, Pittsburgh, PA in press).
21. Anton A. Darhuber, Sandra M. Troian, Jeffrey M. Davis, Scott M. Miller, and Sigurd Wagner, J. Appl. Phys. **88**, 5119 (2000).
22. H. Gokan, S. Esho, and Y. Ohnishi, J. Electrochem. Soc. **130**, 143 (1983).
23. C. Harrison, M. Park, P. M. Chaikin, R. A. Register, and D. H. Adamson, J. Vac. Sci. Technol. B **16**, 544 (1998).